Local Cyclic Voltammetry of a Langmuir-Blodgett Film on Water

Veronika Urbanová,[a] Tomáš Bartl,[a] František Vavrek,[b] Ondřej Pačes,[a] Lubomír Pospíšil,[a,b] and Josef Michl[a,c]*

[a] *Institute of Organic Chemistry and Biochemistry Czech Academy of Sciences, Flemingovo nám. 542/2, 160 00 Prague, Czech Republic;*

[b] *J. Heyrovský Institute of Physical Chemistry, Czech Academy of Sciences, Dolejškova 2155/3, 182 23 Prague 8, Czech Republic;*

[c] *Department of Chemistry, University of Colorado, Boulder, Colorado 80309-0215, United States*

*E-mail: josef.michl@colorado.edu

Abstract

An electrochemical Langmuir-Blodgett trough that permits an examination of local redox processes in a layer floating on the surface of water with an STM-tip ultramicroelectrode has been constructed and tested on a layer of 1,1´-dicarbooctadecyloxyferrocene.

Introduction

Electrochemical investigation of ultrathin compact 2-D layers has a long history, starting with a report of adsorption of a solute at a mercury-water interface by Brdička[1] in 1942. A rigorous theory of electron transfer to an adsorbate was developed by Laviron,[2] and much work was summarized in reviews.[3,4] Scanning tunneling methods were applied,[5,6] and electron transfer from surface attached ferrocene derivatives was examined as a function of distance from a metallic electrode.[7,8] However, as far as we know, there is no previous study of electron transfer based on contacting an LB monolayer at a solution-air interface with an STM-type tip.

We report the design and construction of an electrochemical Langmuir-Blodgett (LB) trough that permits a local probing of redox processes in two-dimensional samples floating on water surface. The function of the instrument was tested by recording cyclic voltammograms of an LB layer of a ferrocene derivative carrying two C_{18} chains.

Motivation. The need for the instrument arose after the recent successful synthesis of porphene (1, M = 2H),[9] a monolayer of two-dimensional (2-D) porphyrin analog of graphene. This polymer was prepared in an LB trough by slow polymerization of a layer of zinc porphyrin on the surface of an aqueous solution of a chemical oxidant. The process is believed to start with

an oxidation of neutral Zn porphyrin to its radical cation, which then uses its meso position to perform aromatic substitution on a meso position of a neutral neighboring molecule of Zn porphyrin, reversibly forming a C-C bond between the two macrocycles. The process continues until ultimately the reaction 2 C-H - $2e^-$ → C-C + $2H^+$ has occurred at each of the twelve CH bonds present at each porphyrin periphery, forming **1**. The flakes of **1** produced were up to several mm in size, but the single crystalline domains within them were much smaller, with a coherence length of >120 nm. Their size was undoubtedly limited by the large number of polymerization seeds that were produced at numerous locations and random in-plane orientations as diffusion brought the oxidant to the surface layer. Each seed presumably grew until it ran out of available monomer or until its outer perimeter encountered the periphery of neighboring growing domains, defining grain boundaries.

The initially produced polymer is not electroneutral **1**, because an oxidant strong enough to convert a monomeric Zn porphyrin to its radical cation is also capable of injecting positively charged holes into porphene fragments such as dimers, oligomers, and the polymer itself. The initially formed polymer is a heterobilayer consisting of a positively charged layer of **1** attracted by ion pairing to a negatively charged layer of oxidant counterions. Based on a structure secured by grazing incidence X-ray diffraction, if the bilayer is electroneutral overall, 40% of the macrocycles contained in **1** have lost an electron. The strong positive charge present within the partially or fully polymerized porphyrin structures expels most and ultimately all of the initially strongly bound Zn^{2+} cations into the aqueous subphase. After a reductant has been added to return the missing electrons to the polymer, these or other metal cations can be readily reintroduced from solution into the free-base porphene polymer to yield neutral **1** (M = metal).

It was found that a layer of **1** (M = Zn) is an electrical insulator, but a layer doped with holes is a conductor. It thus appeared that it might be possible to reduce the number of seeds and thereby increase the size of domains by contacting the LB monolayer with an ultramicroelectrode, using it as an anode, and oxidizing for a long time. If the injected holes traveled to the perimeter of a domain, they could react there with additional monomer and increase the size of the domain.

We expect that the instrument described below will allow us to ascertain whether such electrooxidation of Zn porphyrin to **1** is feasible and indeed produces large single-crystalline domains. The device may also find other uses, e.g. determination of redox properties of species located on water surface, measurement of concentration of solutes as a function of distance from a liquid surface or interface, or examination of biological membranes. Presently, we test its

operation by investigating the redox behavior of a previously studied[10] LB layer of **2**, a ferrocene carrying two long alkyl chains.

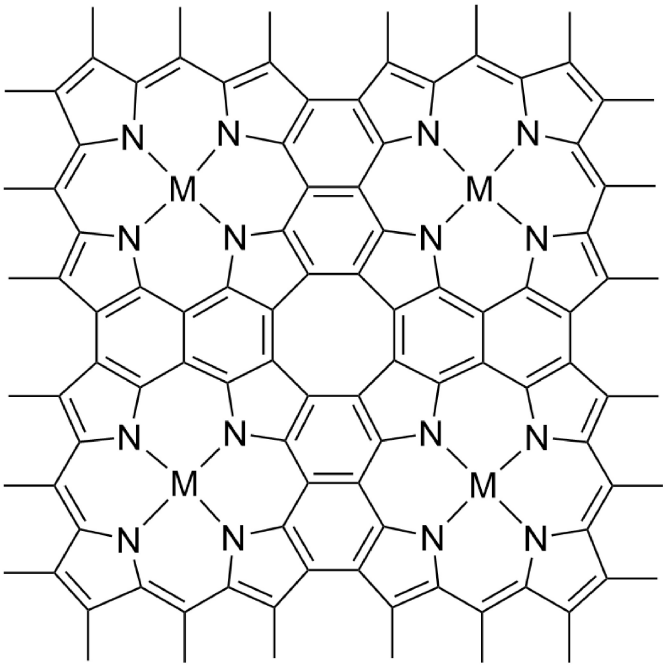

1

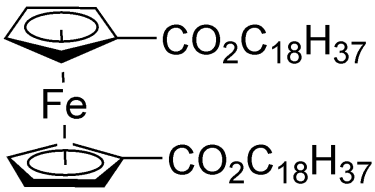

2

Experimental Section

Materials. 1,1′-Dicarbooctadecyloxyferrocene (**2**) was prepared using a literature procedure[10] and purified by column chromatography (alumina, hexane/ethyl acetate 20:1) followed by crystallization from ethanol. Other chemicals were of analytical grade and were used without purification.

Electrochemical Langmuir-Blodgett Trough. Figure 1 provides a schematic representation of the instrument. It consists of a home-made polypropylene LB trough with a Brewster angle microscope (KSV NIMA, MicroBAM, Biolin Scientific), a Wilhelmy plate

balance controlled by a Micro-Processor Interface IU4 module (Nima Technology Ltd.), and a home-made PTFE barrier position control assured by a belt with a hand wheel and a stepper motor. The trough is located inside a home-made Faraday cage and resides on an anti-vibration table (Newport, PG^{TM} Series; Sealed Hole Breadbord). The water level in the trough is kept constant by a linear syringe pump (KdScientific). The potentiostat used for cyclic voltammetry is Ivium CompactStat h10030 (Ivium Technologies BV) equipped with IviumSoft Electrochemical Software.

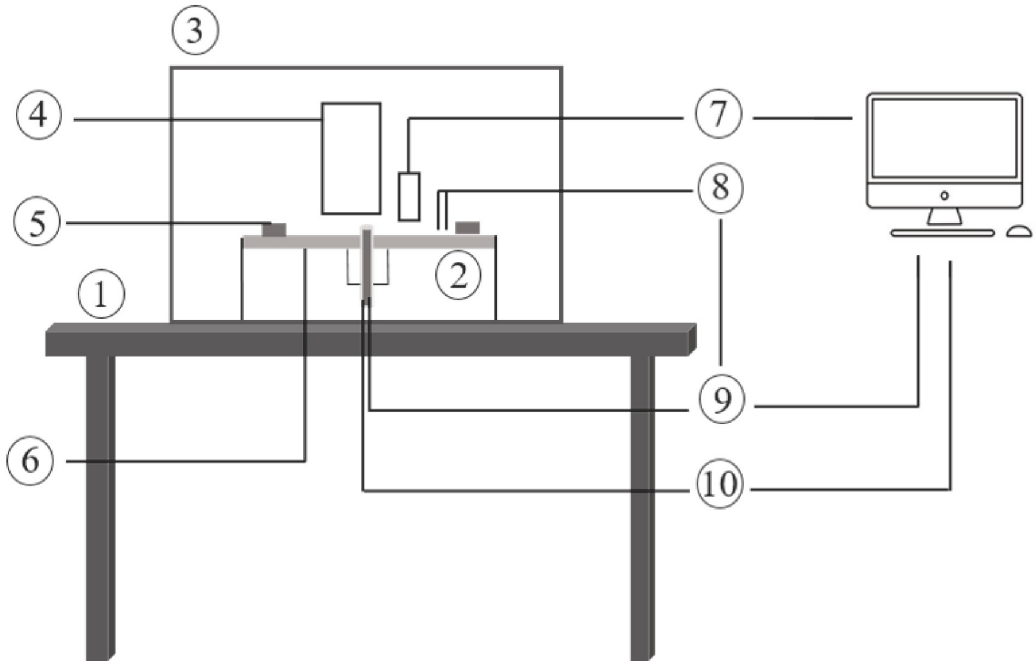

Figure 1. The electrochemical LB trough. 1- anti-vibration table; 2- LB trough; 3- Faraday cage; 4- Brewster angle microscope; 5- movable barriers; 6- water level controller; 7- surface pressure controller; 8- reference and counter electrodes; 9- potentiostat; 10- piezo controller.

A Pt/Ir etched tip and a Ag/AgCl electrode are used as working and reference electrodes, respectively. Near the center of the trough, a vertically mounted piston-style STM-like tip of the working electrode reaches up to the water surface (Figure 2). The vertical position of the working electrode is adjusted coarsely by a microscrew (Mitutoyo Model 153-101, 12 mm travel, 10 µm resolution) and finely by a piezoelectric actuator (Physik Instrumente, Linear Stage P-602, 1SL, 300 µm travel, 1 nm resolution). The micrometer adjustment head and the piezo controller are located under the trough and connected to the piston rod (Figure 2A). The working electrode tip is inside a ~1.5 cm polyoxymethylene (POM) cylinder. The whole piston assembly is placed

inside a housing and sealed with a radial shaft seal for isolation from the liquid, still allowing vertical motion. The insulation of the electrode tip itself was achieved by clamping the PTFE tubing with a piston rod with a threaded end (Figure 2B). The instrument is also equipped with the stainless steel counter electrode of circular shape that is mounted on the electrode piston housing (Figure 2A,B). Its position can be manually changed in vertical direction. Such an arrangement allows the working electrode to be centered and at different distances from the water surface in the LB trough.

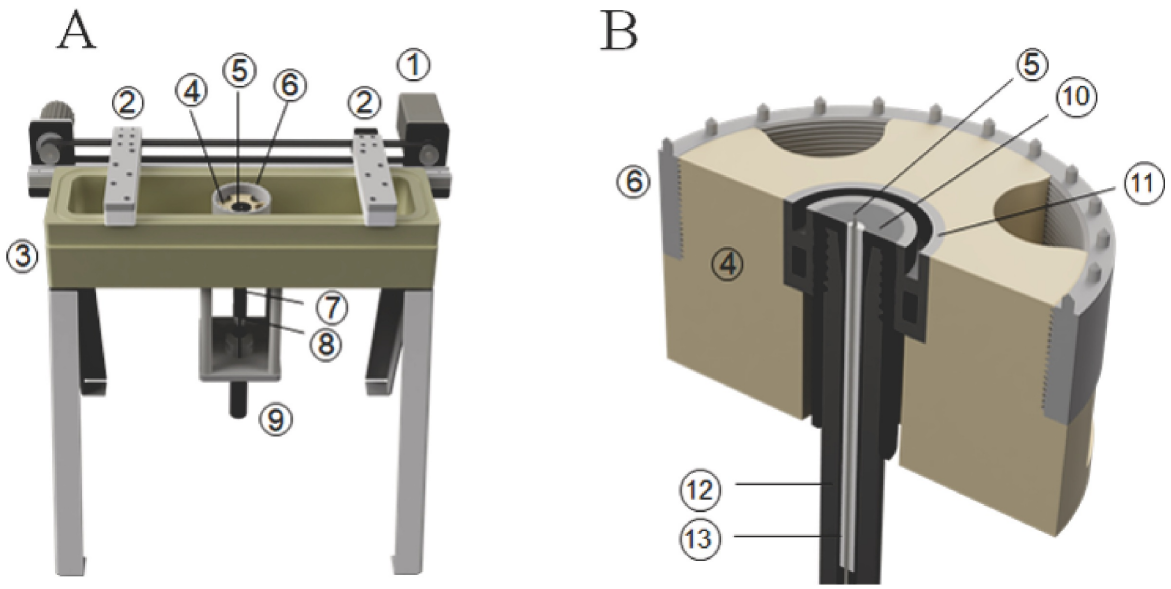

Figure 2. A: LB trough. 1- stepper drive for controlled barrier movement; 2- PTFE barriers; 3- PP trough; 4- electrode piston housing; 5- electrode piston containing PE coated Pt/Ir electrode tip; 6- stainless steel circular counter electrode; 7- piston rod to connect actuator and electrode piston; 8- piezoelectric actuator; 9- micrometer screw. B: Electrode tip detail. 10- electrode piston for movement up and down; 11- rubber seal; 12- steel piston rod with threaded end for sealing purposes; 13-PTFE capillary tubing for electrode tip.

The working electrode tip was made from a 90% Pt-10% Ir alloy wire of 0.25 mm diameter (Goodfellow GmbH, Germany). A ~4 cm long piece of straightened wire was electrochemically AC etched at one end in an aqueous etching solution (1 M $CaCl_2$ and 0.25 M HCl).[11] The shape of the resulting tip was checked under an optical microscope and scanning electron miscroscope (Nova NanoSEM 450, FEI). It revealed a circular cone shape with a pointed apex (Figure 3). The etched wire was then sheathed inside of a PTFE capillary tube (1.5 mm OD/ 0.25 mm ID, Metrohm, Czech Republic), allowing the etched tip to protrude ~2 mm and the other end ~5 mm, providing sufficient wire length for later supply wire soldering. In the

next step, the sheathed etched tip was dipped in molten polyethylene (low-density PE, Sigma-Aldrich). Plasma induced polymer grafting[12] was afterwards used to adjust the contact angle with water to minimize the perturbation of a flat water surface. First, the electrode tip was left in a plasma cleaner at 60 W for 30 s and then it was immediately immersed in 10% aqueous acrylic acid for 1.5 h at room temperature. Finally, the electrode tip was thoroughly washed with ultrapure distilled water. The electrochemical active area was evaluated by cyclic voltammetry on 1 mM potassium ferrocyanide in aqueous 0.1 M Na_2SO_4 and for a collection of tips it ranged from 0.2 to 40 μm^2. Penetration of the water surface with the tip caused neither a perturbation of the surface pressure nor meniscus formation. The water surface remained flat.

In the cyclic voltammograms reported here, the circular counter electrode was not installed and a Pt wire was used instead. It was checked that its location in the aqueous subphase and also the location of the reference electrode had no effect on the results.

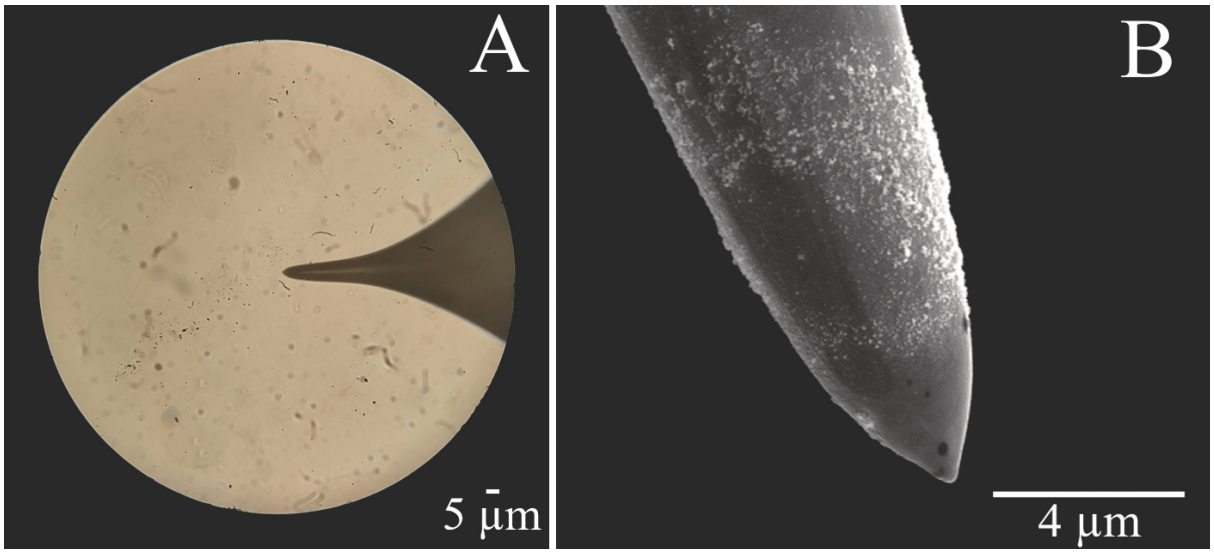

Figure 3. Images of uncoated Pt/Ir electrode tip. A: optical microscope (x1000) and B: SEM (Nova NanoSEM 450, FEI; x15000; 15kV).

LB Layer Preparation. A fresh solution of **2** in chloroform (10 µL; 0.8 mg/mL) was spread from a microsyringe over aqueous 0.1 M NaCl subphase and left for 30 min to evaporate chloroform. The formation of LB film was monitored by surface pressure changes using a Wilhelmy balance.

Results

There are three main variables that determine the appearance of cyclic voltammograms obtained with the new instrument: (i) The mean molecular area (mmA) available to each molecule present in the surface layer, which dictates the layer structure. This is a function of the number of surface molecules present and of the position of the barriers, which selects the surface area covered. (ii) The vertical position of the tip electrode, which controls the fraction of the uncoated surface at its end that is in contact with the LB layer. The position is controlled by the piezo element and the fraction can vary from 0 to 100%. (iii) The nature of the potential sweep. In ordinary anodic cyclic voltammetry, the sweep starts at a low potential well below the redox potential of **2**, proceeds to more positive potentials, and at a selected potential its direction is reversed toward the initial low value. After this is reached, the process can be repeated.

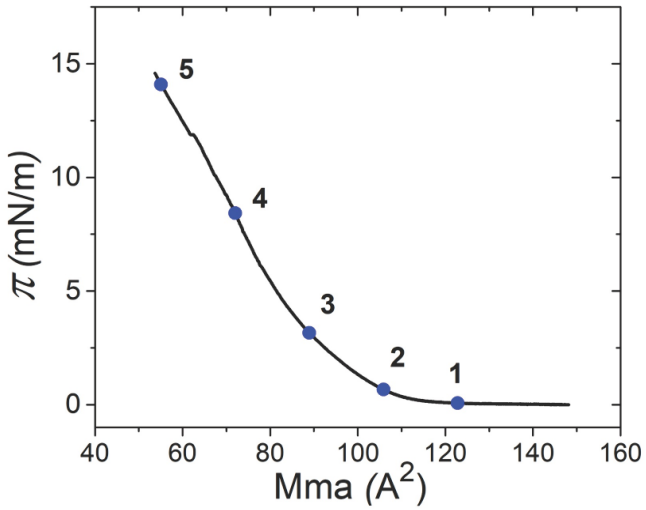

Figure 4. Room-temperature LB isotherm of **2** on aqueous 0.1 M NaCl (surface pressure versus molecular mean area, 0.1 mm/s barrier compression rate).

The LB isotherm of **2** is shown in Figure 4. It has a shape expected for a material forming a stable surface layer. Contact between molecules begins to occur at an mmA equal to 100 - 110 $Å^2$. Figures 5 and 6 show the response of cyclic voltammograms to the variables (i) - (iii). The results were not affected when the atmosphere above the LB trough was replaced with argon.

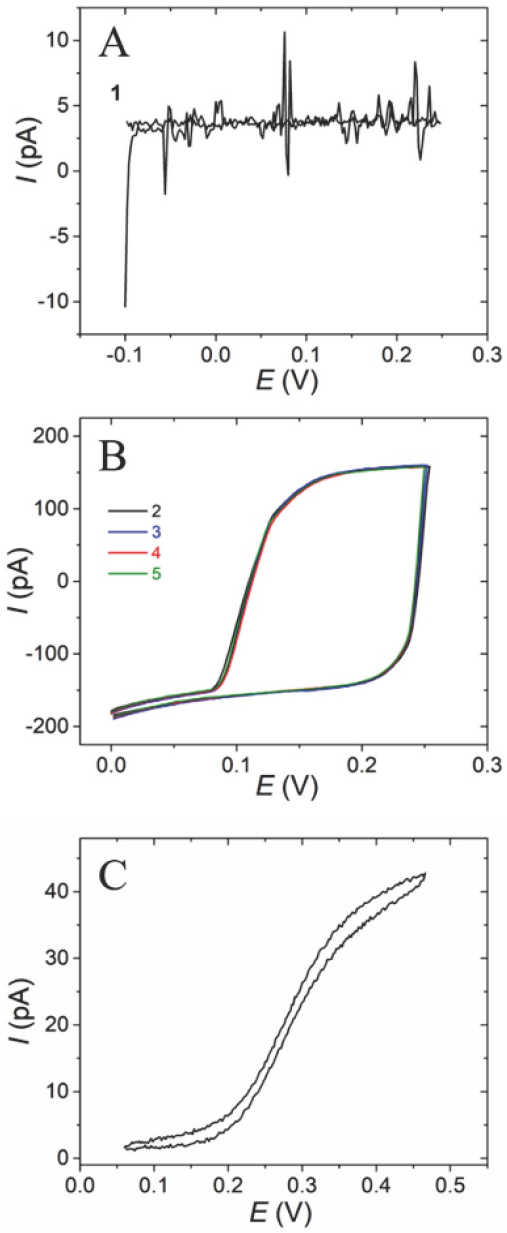

Figure 5. Room-temperature cyclic voltammograms of LB layer of **2** on aqueous subphase containing 0.1 M NaCl using a Pt/Ir tip electrode with an active surface area of 9 μm^2 (5 mV/s, a Pt wire counter electrode, a Ag/AgCl reference electrode). A: at point 1 in the LB isotherm; B: at points 2 - 5 (Figure 4); C: cyclic voltammogram of **2** (20 µM) in 1,2-dichloroethane recorded at 5 mV/s with Pt ultramicroelectrode (⌀25 µm) as working electrode, a Pt wire and a Ag/AgCl as counter and reference electrodes, respectively.

(i) Figure 5 shows cyclic voltammograms recorded under conditions where 100% of the 9 μm^2 active surface area of a Pt-Ir tip is in contact with the LB layer and the reversal potential is close to +0.25 V. They were obtained at five different mmA values, shown in Figure 4 and labeled 1 (Figure 5A) and 2 - 5 (Figure 5B). They show strong hysteresis, which is absent in an ordinary cyclic voltammogram obtained in a bulk solution in 1,2-dichloroethane (Figure 5C). At point 1, the currents are smaller than the noise, whereas at smaller mmA values strong noise-free signals appear and are identical for points 2 - 5.

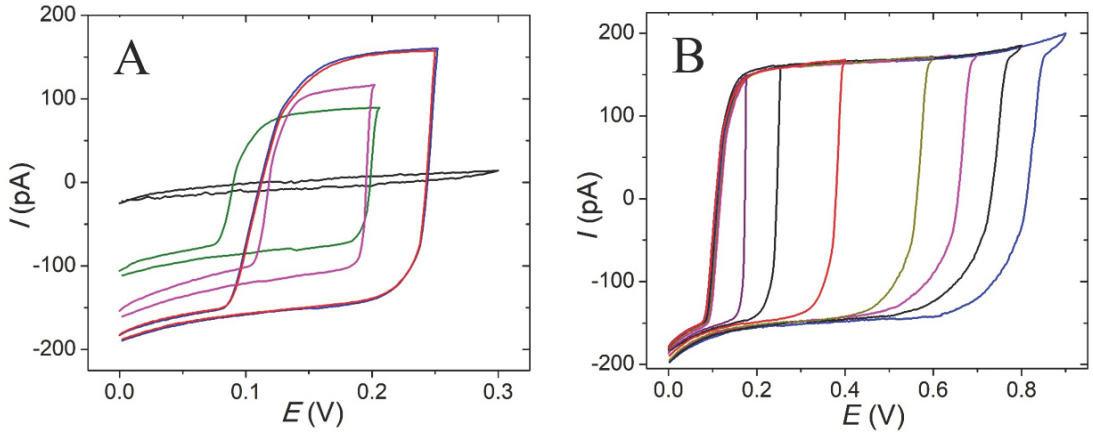

Figure 6. Cyclic voltammograms of 2 obtained in the electrochemical LB trough. A: Cyclic voltammograms during upward motion of the tip using the piezo element, in steps of 1 nm after initial contact with the LB layer. Black, no contact between tip and the organic layer; green, initial contact; magenta, deeper intrusion into the layer; red, full insertion into the layer; blue, further insertion. B: Cyclic voltammograms obtained at different reversal potentials.

(ii) Figure 6A displays cyclic voltammograms for an LB layer with mmA corresponding to point 4 in Figure 4 and a reversal potential of 0.2 - 0.3 V, obtained at different vertical positions of the tip. When the tip anode is positioned too low beneath the water surface and only is in contact with the bulk solution, all that is observed is a small charging current. As the anode is gradually raised sufficiently for contact with the LB layer, a cyclic voltammogram appears with a gradually increasing amplitude, until it reaches a limiting value beyond which further minor increases of the vertical position of the tip make no difference.

(iii) Figure 6B shows cyclic voltammograms obtained for a series of choices for the reversal potential. They were obtained at mmA point 4 in Figure 4, with the active tip of the electrode high enough that further elevation of the tip no longer makes any difference.

All of the cyclic voltammograms obtained under conditions where the electrode tip is in contact with the LB layer exhibit a redox potential of ~0.1 V. At more positive potentials,

electron flow depends on the direction of voltage sweep. When the potential increases, electrons flow from the LB layer into the electrode (anodic wave, oxidation of the LB layer), and when it decreases, current does not flow. When the vertical position of the electrode is in the limiting region where cyclic voltammograms are not affected by its exact location, the current is about 300 pA. The switch from an anodic current to no current is essentially instantaneous upon sweep reversal, except above ~0.6 V, where there is a little hesitation before the current drops to zero upon sweep reversal. At potentials less positive than ~0.1 V, there is no Faradaic current.

Discussion

A simultaneous consideration of Figures 4 and 5 shows that at mmA values in excess of 110 $Å^2$ the surface concentration of **2** and the rate of its surface diffusion are too low to detect its anodic oxidation at the tip of our electrode (point 1 in Figure 4). As soon as a compact layer begins to form, anodic oxidation of Fe(II) to Fe(III) is detectable easily (**2** to $\mathbf{2}^{+\bullet}$, points 2 - 5 in Figure 4) when the vertical position of the electrode is appropriate. Figure 6 demonstrates that the anodic process indeed involves the LB layer and is not due to a presence of a significant amount of **2** in the bulk solution just below the surface.

As might be expected, anodic oxidation of the closely packed LB layer of **2** occurs at less positive potentials than that of the individual molecules of **2** in solution. However, in view of the vastly different properties of water and 1,2-dichloroethane we hesitate to draw any conclusions about layer structure from the 150 - 200 mV difference.

Several other observations are noteworthy:

(i) The observed cyclic voltammograms are essentially identical at points 2 - 5 and are not affected by an order of magnitude increase in the surface pressure, which reduces the mmA by a factor of two. Either the packing is such that the increased pressure packs the alkyl chains closer together without bringing the ferrocene heads closer to each other, or the rate of molecule-to-molecule charge jumps does not limit the observed currents.

(ii) The shape of the anodic oxidation curve is unusual in that it shows a clear break in the slope when the anodic voltage reaches a value of about 100 mV above the rise onset, at which the rising current has reached about 2/3 of its limiting value. It appears that nature of the dominant current limiting reaction step changes at this point. No such behavior is observed on a cyclic voltammogram recorded in bulk solution, and it appears likely that it is associated with some structural change in the LB layer.

(iii) The result that is perhaps the most relevant for the planned study of porphene is the

dependence of the cyclic voltammetric curve on the vertical position of the tip, which is covered by an insulating layer except for its very top. Since the solubility of **2** in water is negligible, it is no surprise that no current flows at any potential when the top of the tip is far below the LB layer floating on the surface (Figure 6). As the tip is raised, its very end touches the LB layer, contact is established, and cyclic voltammetry signal appears. The current is proportional to the area of the tip that is covered with the LB film and is initially small. As the tip is raised, the covered area increases and so does the current. Finally, all of the part of the tip that is not coated with polyethylene is covered with the LB film and additional upward motion of the tip has no effect. During the stepwise vertical rise of the tip, the current at the starting potential of the voltammograms becomes increasingly more negative (green, magenta, red and blue curves in Figure 6A). This is attributed to a change of the double layer structure and capacity. These correspond initially to an aqueous medium containing chloride anions, and gradually convert to a situation appropriate for contact with the organic phase of the LB layer. The change of dielectric permitivity and double layer capacity has a substantial effect on the charging current (the baseline) observed as the potential changes from the starting value to the onset of the oxidation current.

(iv) Unlike the cyclic voltammogram of **2** taken on an ultramicroelectrode in bulk solution, which appears to be perfectly reversible (Figure 5C), that of the LB layer shows considerable hysteresis (Figure 5B). Whereas the anodic wave corresponding to the oxidation of ferrocene to ferricinium (Fc^+) is clearly observed with a half-wave potential at ~0.1 V, the corresponding reverse wave for a reduction of Fc^+ back to ferrocene is absent. We conclude that the more strongly hydrophilic positively charged Fc^+ species is rapidly extracted into the aqueous phase, probably in the form of micelles. Only at the most positive potentials, when its forms the fastest, is the rate of its diffusion out of the LB layer insufficient to suppress all observation of its reduction. A similar behavior has been observed during the voltammetry of a microdroplet of nitrobenzene containing ferrocene derivatives that was in contact with an aqueous solution.[13,14]

Conclusions

The new electrochemical instrument works as intended and the LB layer of **2** behaves according to expectations. It has now become possible to perform local examinations of redox processes in an LB layer in its native state at the surface of water, and attempts to synthesize **1** electrochemically can proceed.

Acknowledgement. This work was supported by Czech Science Foundation grant 20-03691X and Institute of Organic Chemistry and Biochemistry, RVO: 61388963. We acknowledge a helpful discussion of the observed electrochemistry with Profs. J. Janata (Georgia Tech) and M.V. Mirkin (CUNY) and of oxygen plasma chemistry with Dr. T. Michl. We acknowledge Milan Mašát for SEM imaging.

References

1. Brdička, R. The polarographic behavior of riboflavin. II. The adsorption of the reduction products and their oscillographic investigation. *Z . Elektrochem.,* **1942,** *48*, 278-686.

2. Laviron, E. General expression of the linear potential sweep voltammogram in the case of diffusionless electrochemical systems. *Electroanal. Chem.* **1979,** 19-28.

3. Goldenberg L. M., Use of electrochemical techniques to study the Langmuir-Blodgett films of redox active materials. *Russian Chemical Reviews,* **1997**, *66*, 1033-1052.

4. Eckermann, A. L.; Feld, D. J.; Shaw, J. A.; Meade,T. J. Electrochemistry of redox-active self-assembled monolayers. C*oordination Chem. Rev*. **2010**, *254*, 1769-1802.

5. Ricci, A. M.; Calvo, E. J.; Martin, S.; Nichols, R. J., Electrochemical scanning tunnelling spectroscopy of redox-active molecules bound by Au-C bonds, *J. Am. Chem. Soc*. **2010,** *132*, 2494-2495.

6. Salvatore, P.; Hansen, A. G.; Moth-Poulsen, K.; Bjørnholm, T. ; Nichols, R.J.; Ulstrup, J., Voltammetry and in situ scanning tunnelling spectroscopy of osmium, iron, and ruthenium complexes of 2,2′:6′,2″-terpyridine covalently linked to Au(111)-electrodes. *Phys. Chem. Chem. Phys*. **2011**, *13*, 14394-14403.

7. Smalley, J. F.; Feldberg, S. W.; Chidsey, Ch. E. D.; Linford, M. R.; Newton, M. D.; Liu, Y.-P. The kinetics of electron transfer through ferrocene-terminated alkanethiol monolayers on gold. *J. Phys. Chem*. **1995**, *99*, 13141-13149.

8. Chidsey, C. E. D.; Bertozzi, C. R.; Putvinski, T. M.; Mujsce, A. M. Coadsorption of ferrocene-terminated and unsubstituted alkanethiols on gold: electroactive self-assembled monolayers. *J. Am. Chem. Soc.* **1991**, *112*, 4301-4306.

9. Magnera, T. F.; Dron, P. I.; Bozzone, J. P.; Jovanović, M.; Rončević, I.; Tortorici, E.; Bu, W.; Miller, E. M.; Miller, E. M.; Rogers, C.; Michl, J. Porphene and porphite as porphyrin analogs of graphene and graphite. *Nat. Comm.*, in press. ChemRxiv. Cambridge: Cambridge Open Engage; 2023, https://doi.org/10.26434/chemrxiv-2022-t84kd-v3.

10. Deschenaux, R., Megert, S., Zumbrunn, C., Ketterer, J., Steiger, R., Organized molecular films from new ferrocene-containing molecular units. *Langmuir* **1997**, *13*, 2363-2372.

11. Pobelov, I. V. *Electron Transport Studies – An Electrochemical Scanning Tunneling Microscopy Approach*, PhD dissertation, RWTH Aachen University, Nordrhein-Westfalen, Germany, 2008.

12. Gupta, B., Hilborn, J. G., Bisson, I., Frey, P. Plasma-induced graft polymerization of acrylic acid onto poly(ethylene terephthalate) films. *J. Appl. Polym. Sci.* **2001**, *81*, 2993-3001.

13. Natakani, K.; Wakabayashi, M.; Chikama, K.; Kitamura, N. Electrochemical studies on mass transfer of ferrocene derivatives across a single-nitrobenzene-microdroplet/water interface. *J. Phys. Chem.* **1996**, *100*, 6749-6754.

14. Aoki, K.; Tasakorn, P.; Chen, J. Electrode reactions at sub-micron oil | water | electrode interfaces. *J. Electroanal. Chem.*, **2003**, *542*, 51-60.